

# Two Lectures on QCD as a String Theory

Charles Thorn

*University of Florida*

1. Hadronic Stringiness
2. Planar QCD as a Worldsheet System

# 1 Outline

## I. Hadronic Stringiness

1. Experimental evidence for a hadronic string model
  - a) Linear Regge Trajectories
  - b) Regge Behavior and  $\infty$  hadronic size
  - c) “Narrow” resonance dominance
2. Lightcone String explanation of these features
3. Large  $N_c$ 
  - a) Planar diagrams
  - b) Resonances are stable ( $\Gamma = O(1/N_c)$ )
  - c) Rules for planar QCD Feynman diagrams

## II. Worldsheet system for planar ( $N_c = \infty$ ) QCD

1. QFT Lightcone Worldsheet
2. Ising spin rep of multi-loops: ( $D+1$ ) dimension
3. Cubic Gauge Vertex on Worldsheet
4. Quartic vertices from cubics
5. Ultraviolet divergences
6. Renormalization on the Worldsheet
7. Conclusions

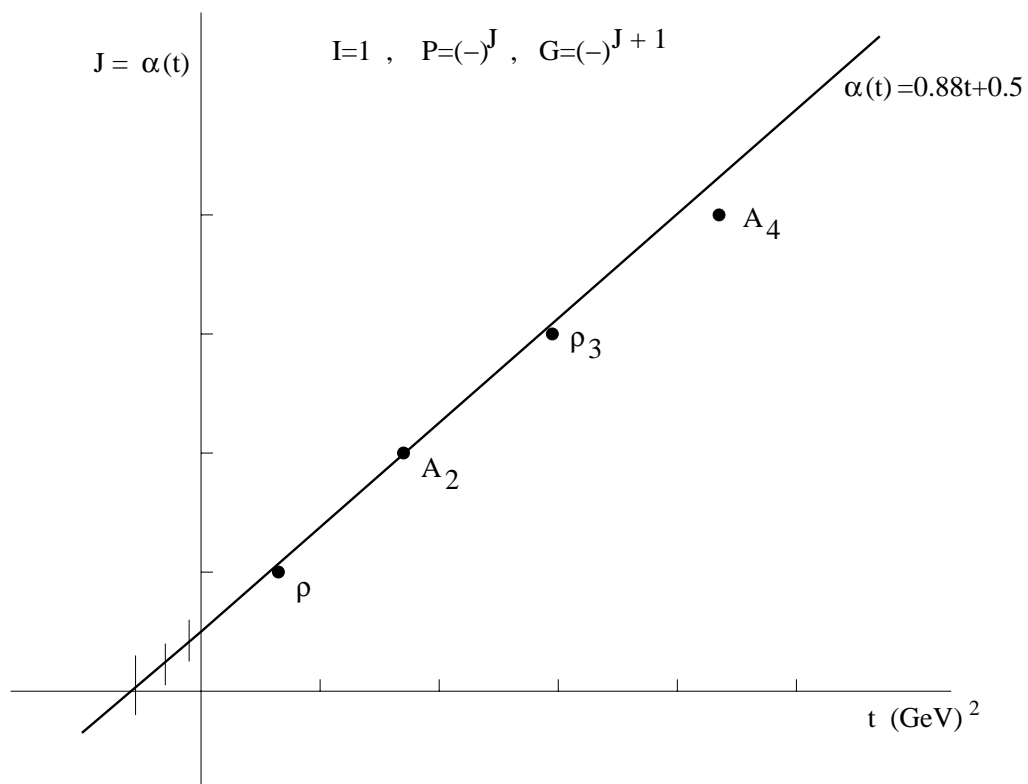
## 2 Why bother?

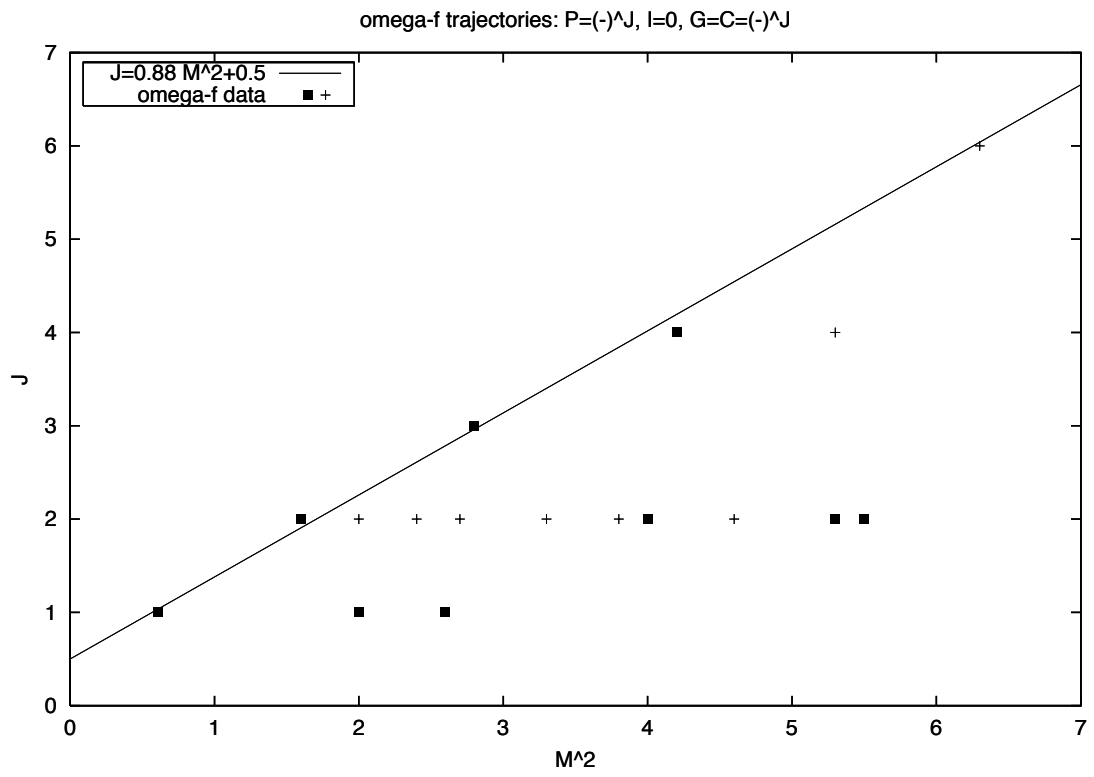
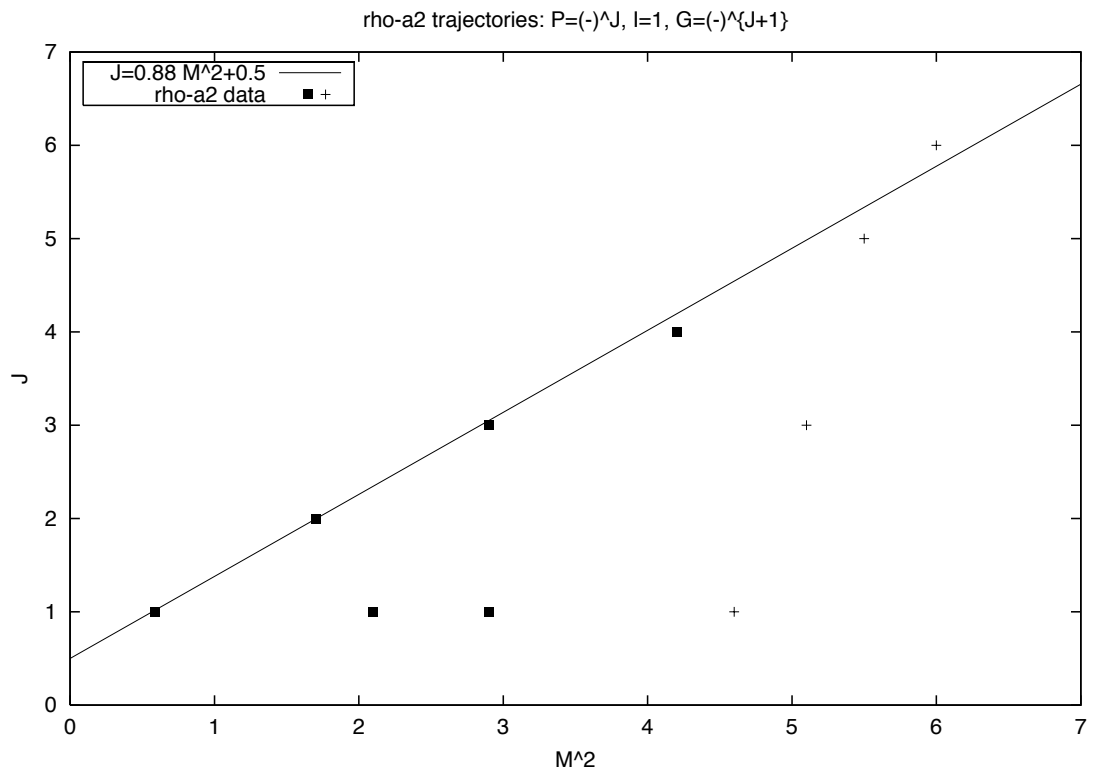
1. The phenomenology of mesons and baryons includes many “stringy” aspects. QCD should eventually be able to explain them. Establishing a string description of QCD may be the best way to accomplish this.
2. String theory is not just a theory of quantum gravity and everything else: e.g. from AdS/CFT correspondence we know some string theories are equivalent to flat space quantum field theories. A string theory equivalent to QCD would finally confront string ideas with reams of experimental tests much more stringent than may ever be obtained for string’s quantum gravity/TOE application.
3. Proper form of string theory still a work in progress. Since sound formulations of QFT already exist, each string/QFT duality throws new light on this project.
4. Experience shows that when a theory actually makes contact with nature, experimental feedback illuminates aspects of the theory undreamt of by its most brilliant practitioners.

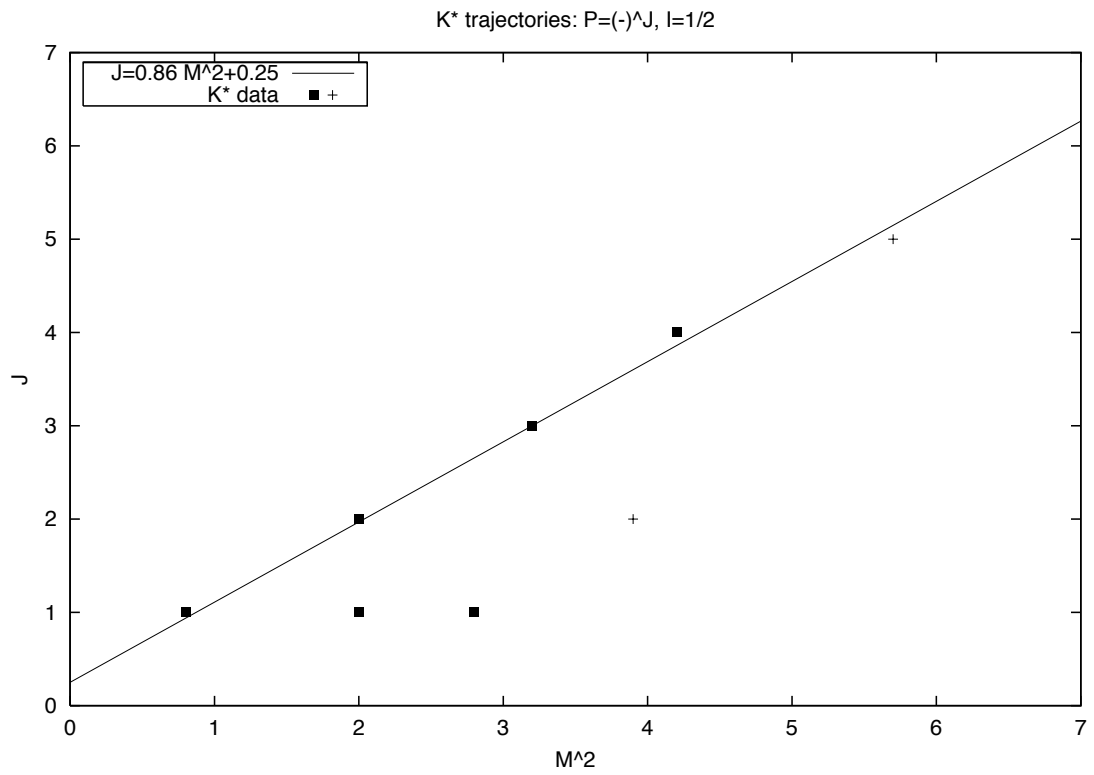
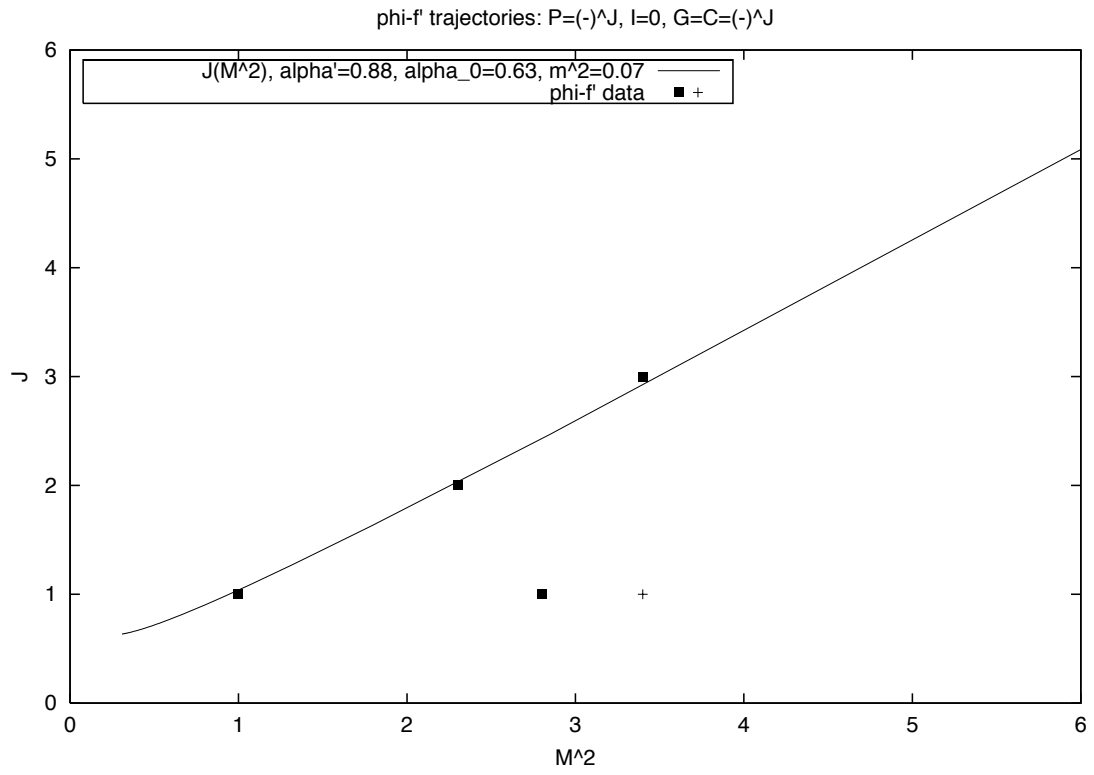
# 3 I: Hadronic Stringiness

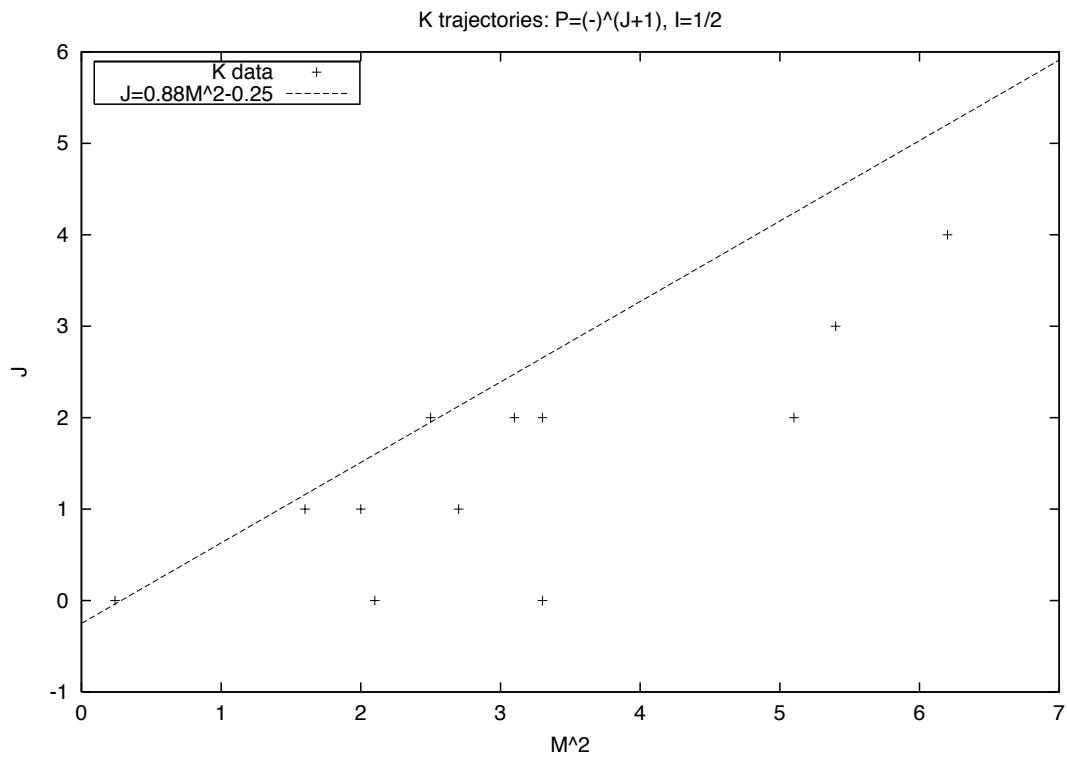
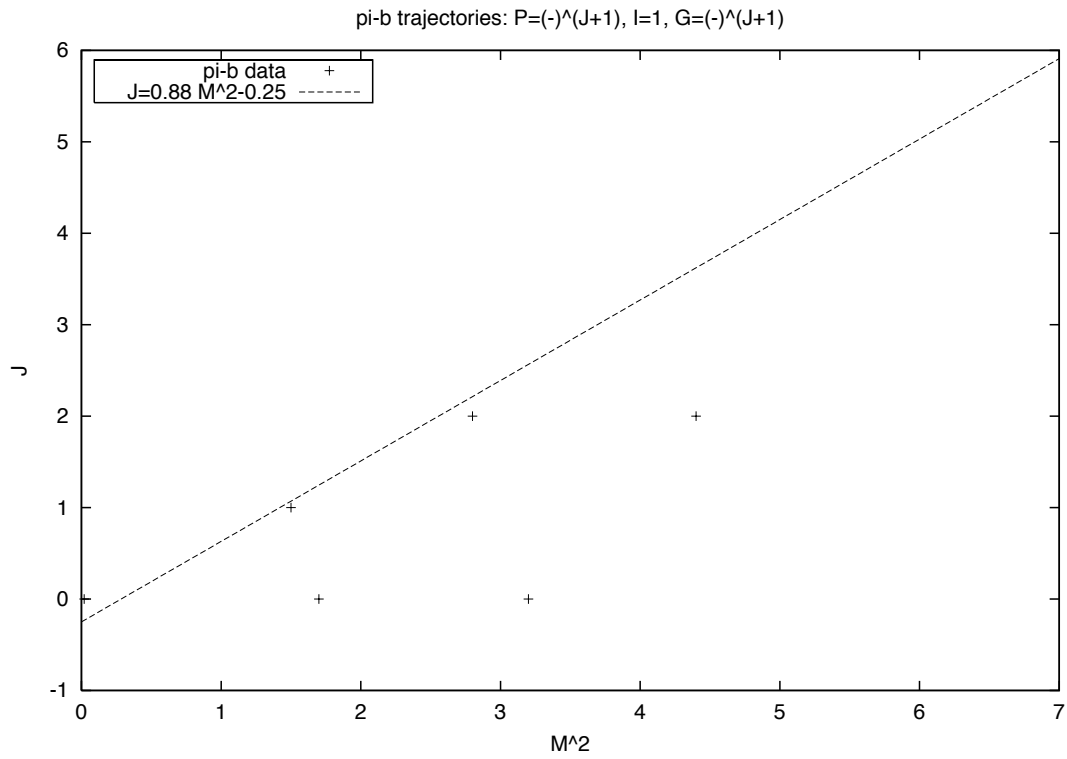
## 3.1 Phenomenological Stringiness

1. Hadrons fall on approximately linear Regge trajectories

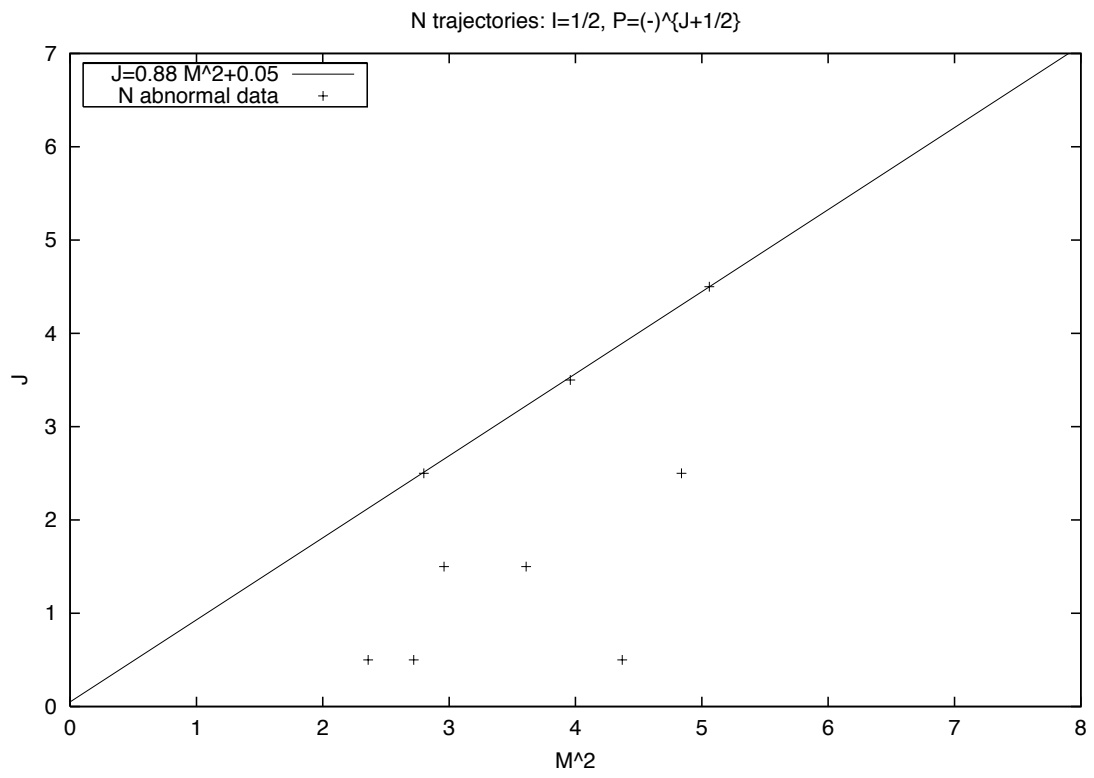
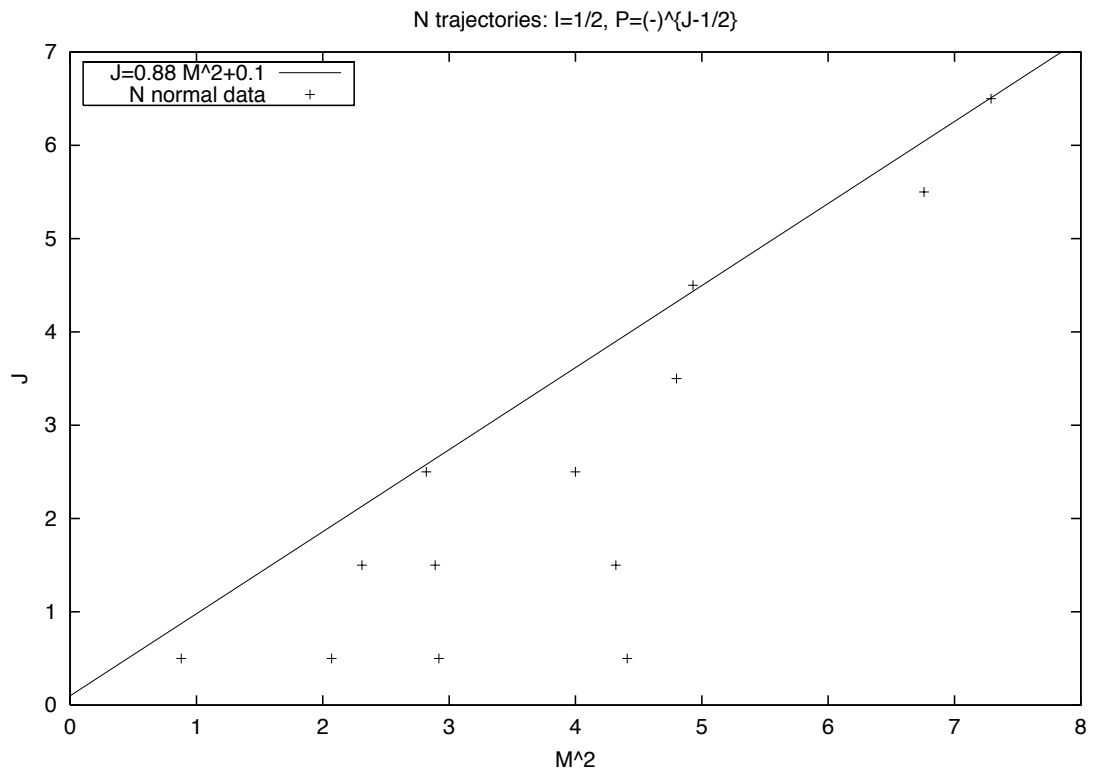


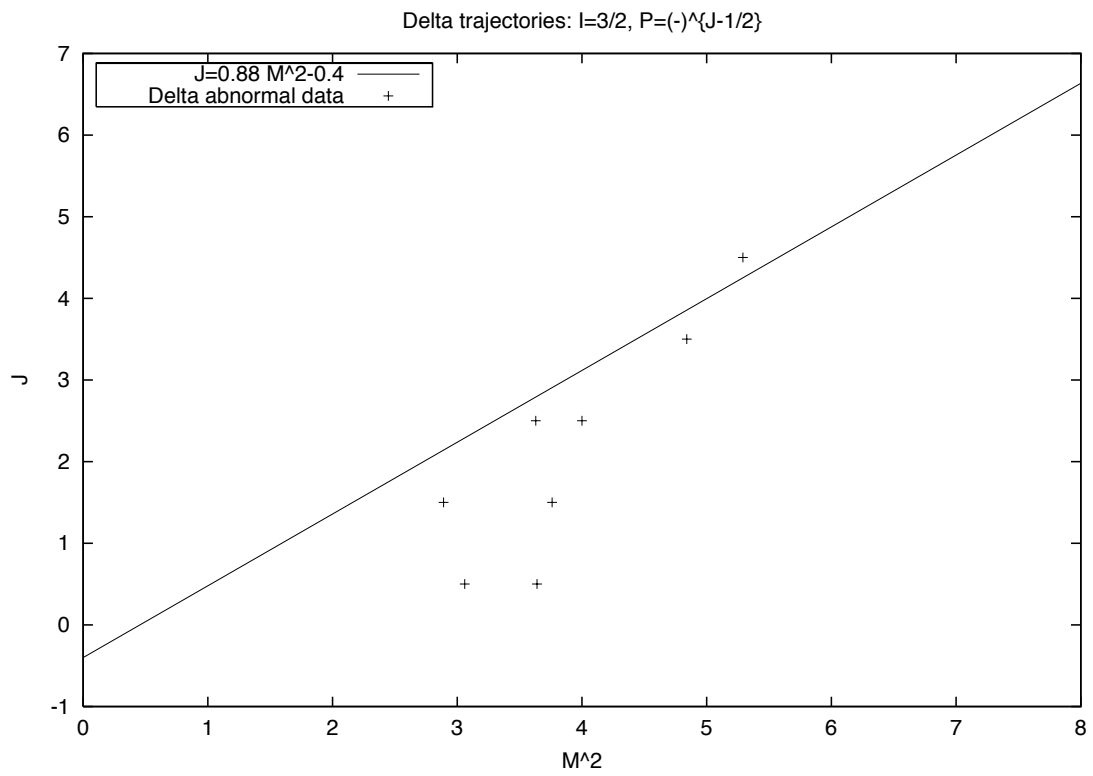
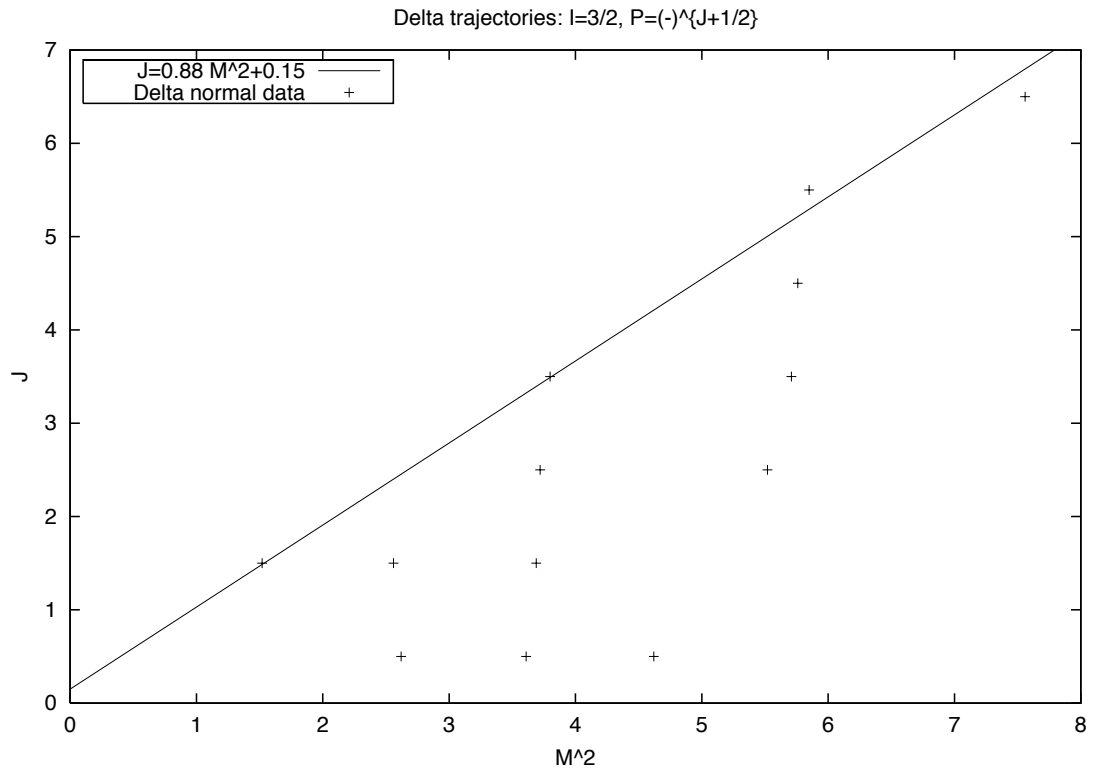


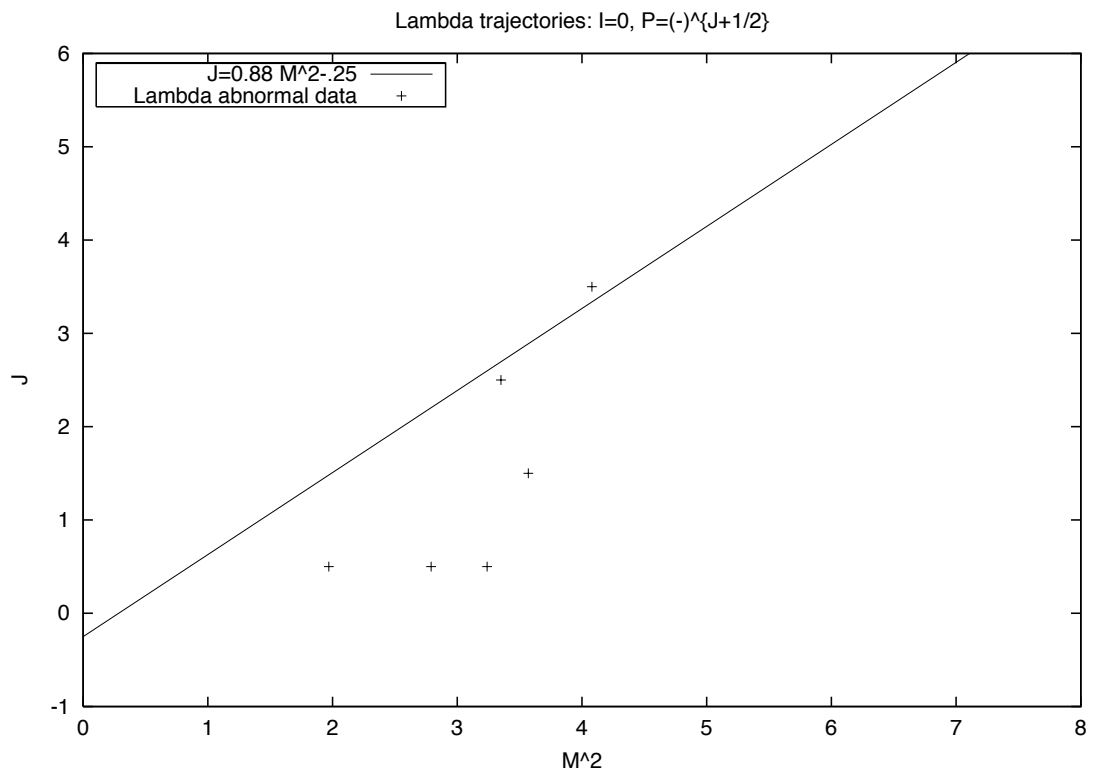
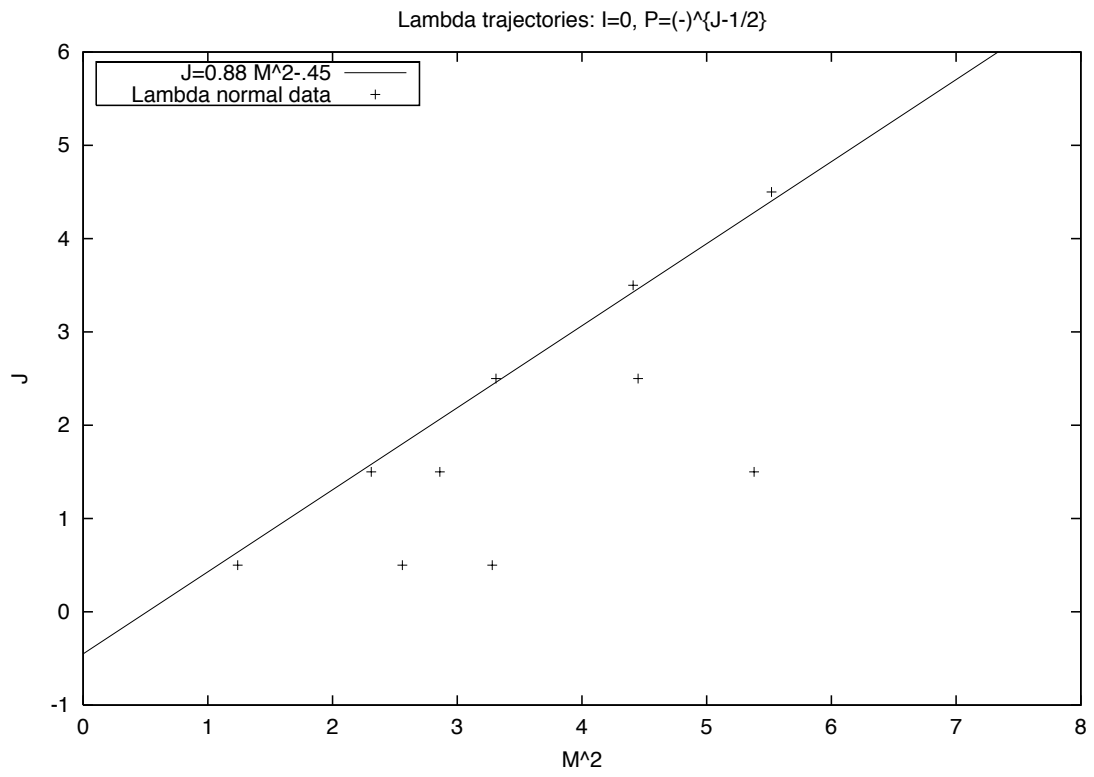


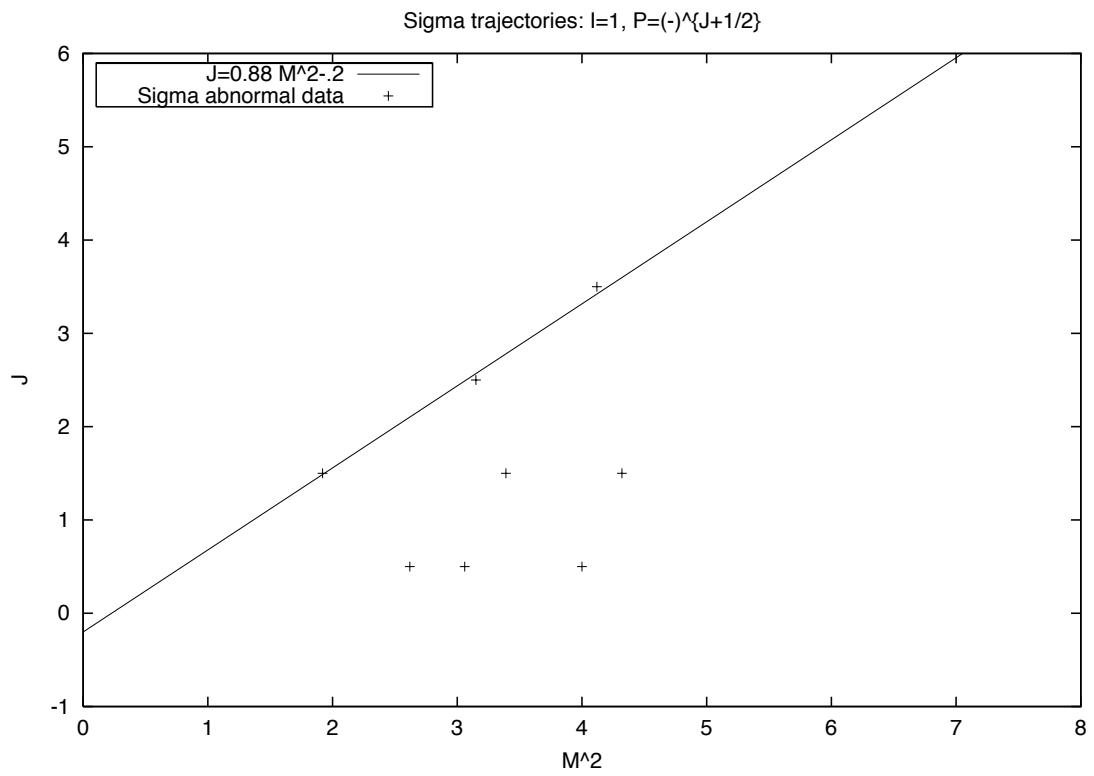
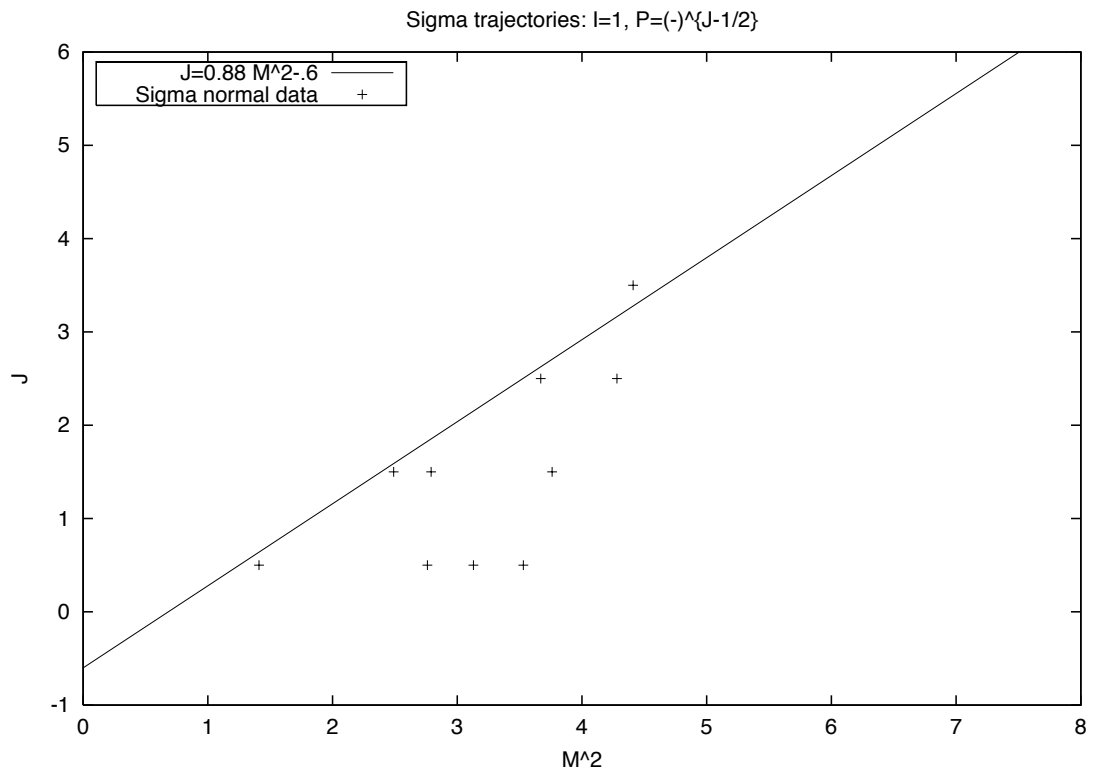






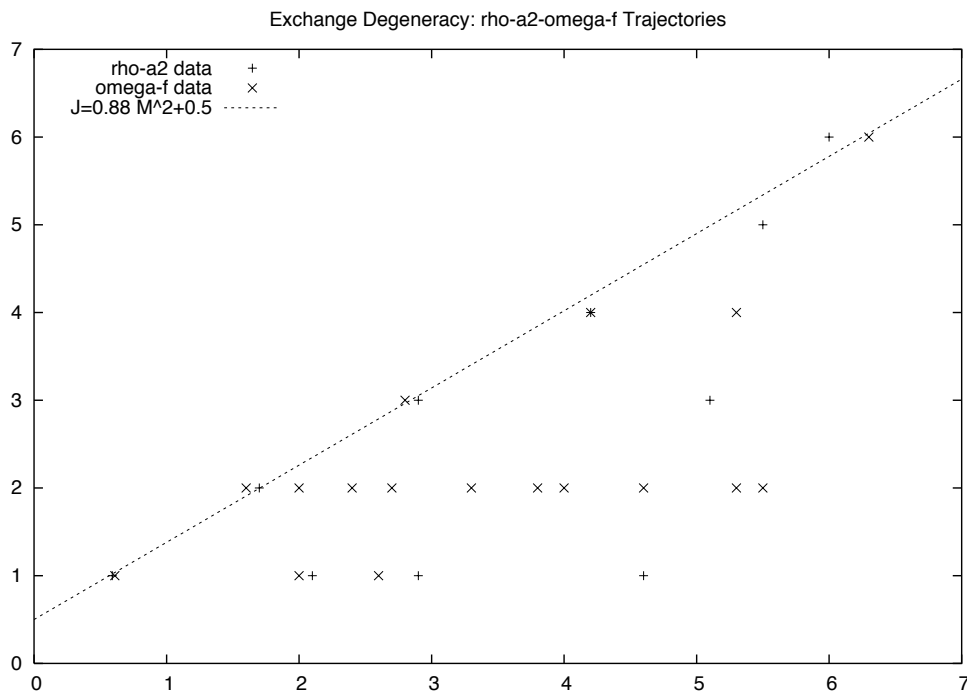






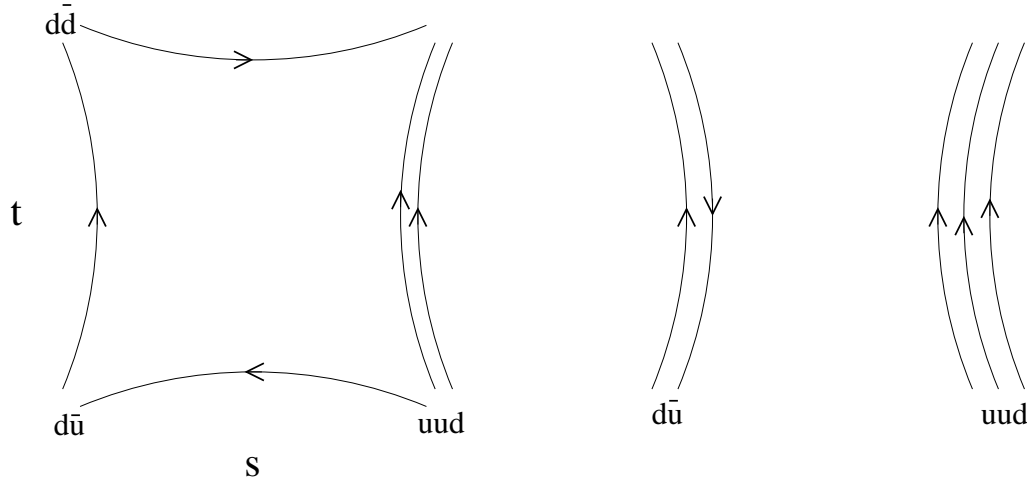
## 2. Exchange degeneracy: Temporary Suspension of Statistics Restrictions

On general grounds particles of even and odd  $J$  should lie on distinct Regge trajectories. (This is because of exchange forces in systems of identical constituents.) Plots of the data indicate that these trajectories are nearly degenerate:



This suggests that “exchange forces” are weak and encourages neglecting them in first approximation. (Exchange degeneracy) This supports an approximate dynamics described by planar Feynman diagrams. Mesons as open strings.

3. Hadronic scattering amplitudes show clear cut Regge behavior in processes in which “Vacuum Quantum Number Exchange” is excluded: e.g.  $\pi^- + p \rightarrow \pi^0 + n$ . For  $s \rightarrow \infty$



$$A(s, t) \sim \beta(t) s^{\alpha(t)}$$

$$s = -(p_- + p_p)^2 > 0, \quad t = -(p_0 - p_p)^2 < 0$$

The  $t$  dependence of the power of  $s$  can be fit. Consistent with a straight line passing through the resonances  $\rho, \rho_3, \dots$  on the The Regge trajectory  $\alpha(t)$ .

Note: Vacuum exchange must be removed. It is dominated by glueball (“Pomeron”) exchange, and while these may be controlled by Regge trajectories, their  $\alpha'_{\text{Pom}}$  is small near  $t = 0$ . Because the Pomeron intercept is near unity these processes swamp  $\rho$  exchange, unless vetoed by charge exchange.

4. Resonance/Regge duality in the same Pomeron-free processes.

Dolen, Horn and Schmid modelled  $A(s, t)$  as a sum of narrow resonance shapes using resonance data from phase shift analyses. They showed that the Regge form described this resonance model in an average way and extracted an  $\alpha(t)$  compatible with that directly measured.

This encouraged the search for narrow resonance models of Regge behavior by Ademollo, Rubinstein, Veneziano, and Virasoro that culminated in Veneziano's proposed amplitude for  $\pi + \pi \rightarrow \pi + \omega$

$$A(s, t) = g^2 \frac{\Gamma(-\alpha' s - \alpha_0) \Gamma(-\alpha' t - \alpha_0)}{\Gamma(-\alpha'(s + t) - 2\alpha_0)}$$

and the rest is the history of string theory. Exchange degeneracy is reflected in the absence of  $u$  channel singularities in  $A(s, t)$ .

## 3.2 Why this phenomenology is stringy.

Worldsheet Description of String

Coordinates and Momenta of String

$$x^\mu(\sigma, t), \quad \mathcal{P}^\mu(\sigma, t)$$

Here  $\mathcal{P}^\mu d\sigma = dp^\mu$  is the energy momentum carried by the element  $d\sigma$  of string.

Nambu-Goto String on the Lightcone:

$$x^+ \equiv \frac{1}{\sqrt{2}}(x^0 + x^3) = t, \quad \mathcal{P}^+ = 1$$

$$S = \int dt \int_0^{p^+} d\sigma \left( \dot{\mathbf{x}} \cdot \mathcal{P} - \frac{1}{2} \mathcal{P}^2 - \frac{T_0^2}{2} \mathbf{x}'^2 \right)$$

$$S \rightarrow \int dt \int_0^{p^+} d\sigma \frac{1}{2} (\dot{\mathbf{x}}^2 - T_0^2 \mathbf{x}'^2)$$

Eq. of Motion for Open String:

$$\begin{aligned} \frac{\partial^2 \mathbf{x}}{\partial t^2} &= T_0^2 \frac{\partial^2 \mathbf{x}}{\partial \sigma^2} \\ \frac{\partial \mathbf{x}}{\partial \sigma} &= 0, \quad \sigma = 0, p^+ \end{aligned}$$



Normal modes:

$$x^k(\sigma, t) = x_0^k + \frac{p^k}{p^+}t + \sqrt{\frac{2}{p^+}} \sum_{n=1}^{\infty} \frac{a_n^k e^{-i\omega_n t} + a_n^{k\dagger} e^{i\omega_n t}}{\sqrt{2\omega_n}} \cos \frac{n\pi\sigma}{p^+}$$

$$\omega_n = T_0 \frac{n\pi}{p^+}, \quad [a_n^k, a_m^{l\dagger}] = \delta_{mn} \delta_{kl}$$

$$H = p^- = \frac{\mathbf{p}^2 + M^2}{2p^+}$$

$$\alpha' M^2 = \sum_{n=1}^{\infty} n \mathbf{a}_n^\dagger \mathbf{a}_n - \frac{D-2}{24}, \quad \alpha' = \frac{1}{2\pi T_0}$$

The mass eigen-states are of form

$$a_{n_1}^{k_1\dagger} \cdots a_{n_l}^{k_l\dagger} |0\rangle$$

with maximal  $J = l$  and

$$\text{mass}^2 = (n_1 + \cdots + n_l)/\alpha'$$

Leading trajectory has minimal mass for fixed  $J = l$ , so  $n_1 = n_2 = \cdots = n_l = 1$ , and

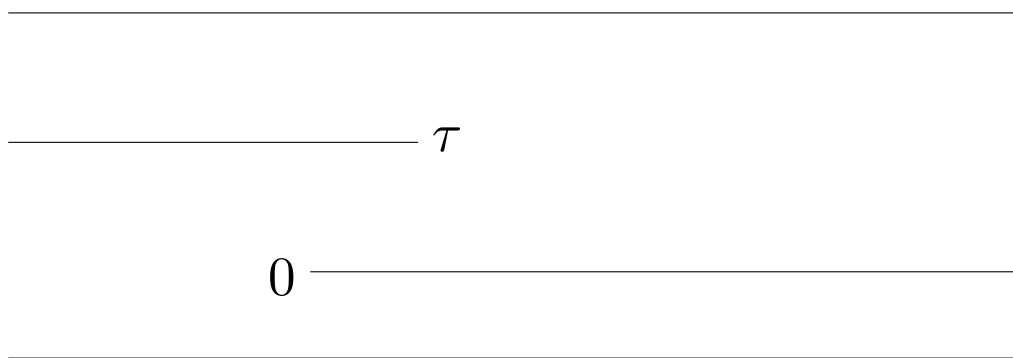
$$\alpha' M^2 = l - (D-2)/24,$$

predicting a linear trajectory

$$\alpha(M^2) = l = \alpha' M^2 + (D-2)/24.$$

Regge Behavior (String has it but Regge behavior is found in other models as well)

Mandelstam showed that with a Light-cone world-sheet of shape  $\Sigma(\tau)$ :



The path integral with free string action

$$A(s, t) = \int_{-\infty}^{\infty} d\tau \int D\mathbf{x} \exp \left\{ -\frac{1}{2} \int_{\Sigma(\tau)} (\dot{\mathbf{x}}^2 + T_0^2 \mathbf{x}'^2) \right\}$$

predicts the Veneziano formula which is Regge behaved.

This is a technically sophisticated calculation, so we turn instead to a simple but peculiar consequence of Regge behavior that is easy to explain with string.

## Infinite Hadronic Size

Near momentum transfer  $t = 0$ ,  $\alpha(t) \approx \alpha' t + \alpha_0$ , so Regge behavior implies a sharp forward peak in  $A$  as a function of  $t$  that shrinks with energy:

$$A \sim C e^{-\alpha' |t| \ln s} \quad (1)$$

This behavior implies the scattered system has an effective size  $R^2 \approx \alpha' \ln s$ .

Take, e.g.,  $p_1^- = 0(s)$ ,  $p_1^+ = O(1/s)$  and  $p_2^\pm = O(1)$ . Then  $s \approx p_1^- p_2^+$ . Then hadron 2 as probed by hadron 1 has a transverse size of  $O(\sqrt{\ln s})$ . But since  $s$  can be arbitrarily large, the light-cone wave function of system 2 must actually have an infinite size.

We can easily see that this peculiar feature is a characteristic of string. For example consider the correlator

$$\begin{aligned} & \langle 0 | (x(p^+, \Delta_t) - x(0, \Delta_t))(x(p^+, 0) - x(0, 0)) | 0 \rangle \\ &= \frac{2}{\pi T_0} \sum_{n=1}^{\infty} \frac{1 - (-)^n}{n} e^{-i\omega_n \Delta_t} \\ &\sim -4\alpha' \ln \frac{\Delta_t}{\alpha' p^+} \end{aligned}$$

We can regard  $\Delta_t$  as the time resolution limited by the uncertainty principle  $\Delta_t > 1/p^-$ , so we get the effective size of the string *ground* state:

$$\Delta x^2 \sim 4\alpha' \ln(2\alpha' p^+ p^-) = 4\alpha' \ln(\alpha' s)$$

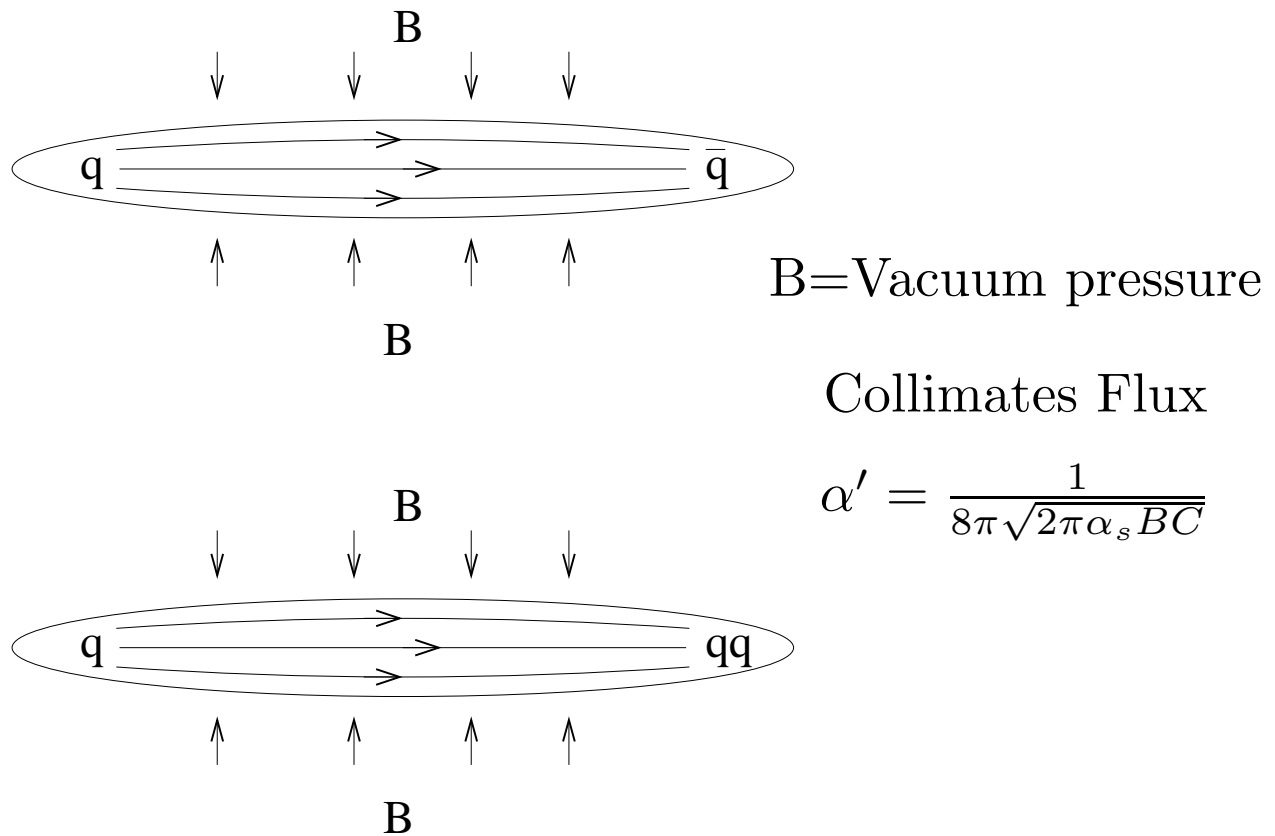
as required by Regge behavior.

It must be emphasized that this infinite size is of one hadron as measured by another hadron. The size of a hadron measured by scattering of a virtual photon is certainly finite. One of the earliest recognized short-comings of the Nambu-Goto string was its failure to explain how a photon will *not* measure an infinite size for the hadron. ( $F_{NG}(q^2) \sim e^{-\infty q^2}$ )

It might be tempting to prefer the bag model of long hadrons as a flux tube of fixed transverse size. But such a picture would not be consistent with Regge behavior and that should probably be regarded as a significant short-coming.

The hadron wave function should embody both features: an infinite size as measured by another hadron but a finite size as measured by form factors.

### 3.3 Long String-like Bags



Bag model states have finite size (good form factors), but won't include the infinite size fluctuations dictated by Regge behavior.

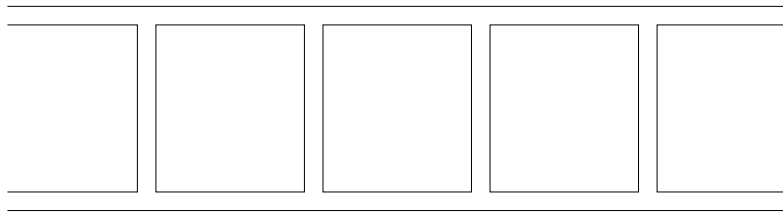
In 1980's Polyakov suggested that a Liouville-like field dependence in the string tension could simulate finite thickness in a way that also allows infinite size fluctuations. More recently this has been realized in the AdS/CFT correspondence of Maldacena.

## Expectations from QCD

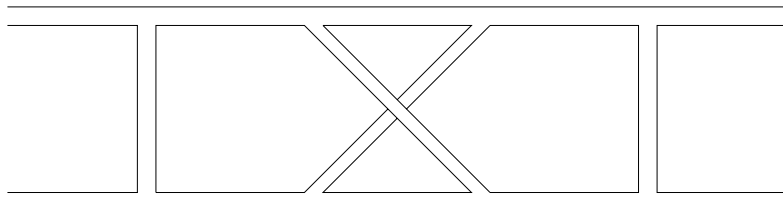
1. Flux tube realization of confinement: Regge trajectories *asymptotically* linear at large mass. Linearity at relatively small mass into negative  $t$  region is puzzling though not inconsistent.
2. Form factors should measure a finite hadron size. High momentum probes should reveal point-like constituents (quarks, gluons). Infinite hadron size as measured by hadron scattering a puzzle.
3. 't Hooft identified a parametric limit  $N_c \rightarrow \infty$  which restricts perturbation theory to planar Feynman diagrams only, and exchange degeneracy is exact in the limit. Corrections to exchange degeneracy are  $O(1/N_c^2)$ .
4.  $N_c \rightarrow \infty$  *and* the hypothesis of confinement imply narrow resonances, i.e.  $\Gamma_{Res} = O(1/N_c)$ .
5. Regge trajectories should not be *exactly* linear, even at  $N_c = \infty$ .

Points 2 and 5 conflict with known string theories. An accurate string description of planar QCD can perhaps explain them.

## 4 $1/N_c$ Basics

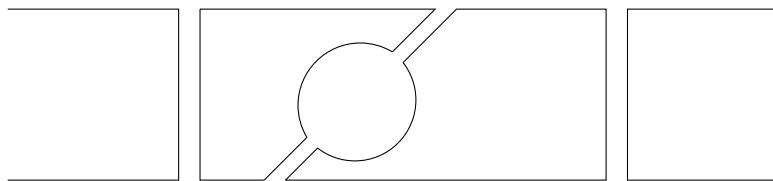


$$O(N_c^3)$$

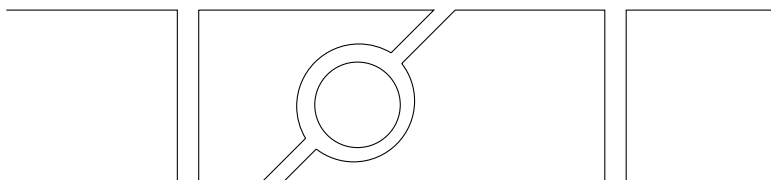


$$O(N_c)$$

So nonplanar complications  $O(1/N_c^2)$ .



$$O(N_c^2)$$



$$O(N_c^3)$$

So Resonance widths  $O(1/N_c)$ .

## 5 Field Theory Limit: $T_0 \rightarrow \infty$

Imaginary  $x^+$ :  $\tau \equiv ix^+ > 0$

$$iS \rightarrow - \int d\tau \int_0^{p^+} d\sigma \frac{1}{2} (\dot{\mathbf{x}}^2 + T_0^2 \mathbf{x}'^2)$$

Field theory limit forces  $\mathbf{x}' = 0$ , freezing almost all worldsheet degrees of freedom.

T Duality:  $(\mathbf{q}', \dot{\mathbf{q}}) = (\dot{\mathbf{x}}, -T_0^2 \mathbf{x}')$

$$\begin{aligned} iS &= - \int d\tau \int_0^{p^+} d\sigma \frac{1}{2} (\mathbf{q}'^2 + T_0^{-2} \dot{\mathbf{q}}^2) \\ &\rightarrow - \int d\tau \int_0^{p^+} d\sigma \frac{\mathbf{q}'^2}{2} \quad \text{for } T_0 \rightarrow \infty \end{aligned}$$

Field theory limit leaves all worldsheet degrees of freedom intact. Still almost none of these degrees of freedom are dynamical!

We shall exploit this fact to *construct* a worldsheet system to reproduce the sum of the planar diagrams of a wide range of quantum field theories.



# 6 QFT Lightcone Worldsheet

Bardakci-Thorn(NPB626:287,2002)

Master Formula for Massless Propagator:

$$\begin{array}{c} T \\ | \\ \mathbf{p}, p^+ \\ | \\ 0 \end{array} = \begin{array}{c} T \\ \square \\ \mathbf{q}(\sigma, \tau) \\ \square \\ 0 \quad p^+ \end{array}$$

$$\exp \left\{ -\frac{T}{2p^+} \mathbf{p}^2 \right\} = \int_{\substack{\mathbf{q}(0, \tau)=0 \\ \mathbf{q}(p^+, \tau)=\mathbf{p}}} DcDbD\mathbf{q} e^{iS_0}$$

$$iS_0 = \int_0^T d\tau \int_0^{p^+} d\sigma \left( b'c' - \frac{1}{2} \mathbf{q}'^2 \right)$$

- Dirichlet b.c.'s. Cf. string in momentum space
- Represent a field quantum as a composite of String Bits
- Total  $p^+ = (\text{Number of bits}) \times m$ .

## Derivation of Master Formula

Define path integral on a lattice:

$$\begin{aligned}
 (\sigma, \tau) &\rightarrow (im, ja) \\
 \int d\sigma d\tau \mathbf{q}'^2 &\rightarrow \frac{a}{m} \sum_{i,j} (\mathbf{q}_{i+1}^j - \mathbf{q}_i^j)^2 \\
 \int d\sigma d\tau \mathbf{b}' \mathbf{c}' &\rightarrow \frac{a}{m} \sum_{i,j} (\mathbf{b}_{i+1}^j - \mathbf{b}_i^j)(\mathbf{c}_{i+1}^j - \mathbf{c}_i^j) \\
 D\mathbf{q} D\mathbf{c} D\mathbf{b} &\rightarrow \prod_{ij} \left( d\mathbf{q}_i^j \frac{d\mathbf{c}_i^j d\mathbf{b}_i^j}{(2\pi)^{d/2}} \right)
 \end{aligned}$$

Recall the formula for Gaussian integration over numbers:

$$\begin{aligned}
 \int dx_1 \cdots dx_n \exp \left\{ - \sum_{ij} x_i A_{ij} x_j - \sum_i B_i x_i \right\} = \\
 \det^{1/2}(\pi A^{-1}) \exp \left\{ - \frac{1}{2} \sum_i B_i x_i^c \right\}
 \end{aligned}$$

where  $2 \sum_j A_{ij} x_j^c + B_i = 0$ .

For Grassmann integration the prefactor is the inverse of that for numbers.

The two prefactors cancel in our master formula.

To get the exponent we just find the stationary point of the action:

$$\begin{aligned} \mathbf{q}'' &= 0, & \mathbf{q}(0) &= 0, & \mathbf{q}(p^+) &= \mathbf{p} \\ \mathbf{q}(\sigma) &= \frac{\sigma}{p^+} \mathbf{p}, & \int d\tau d\sigma \mathbf{q}'^2 &= T \mathbf{p}^2 / p^+ \\ \mathbf{c}(\sigma) &= \mathbf{b}(\sigma) = 0 \end{aligned}$$

Generalization of ghost path integral:

$$\begin{aligned} &\int \prod_{i=1}^{M-1} \frac{dc_i db_i}{2\pi} \exp \left\{ \frac{a}{m} \left[ \frac{b_1 c_1}{\eta} + \frac{b_{M-1} c_{M-1}}{\xi} \right. \right. \\ &\quad \left. \left. + \sum_{i=1}^{M-2} (b_{i+1} - b_i)(c_{i+1} - c_i) \right] \right\} \\ &= \frac{M}{\eta \xi} \left( 1 + \frac{\eta + \xi - 2}{M} \right) \left( \frac{a}{2\pi m} \right)^{M-1} \end{aligned}$$

The original integral corresponds to  $\xi = \eta = 1$ . Thus the modification supplies a factor

$$\frac{1}{\eta \xi} \left( 1 + \frac{\eta + \xi - 2}{M} \right) \tag{2}$$

on each time slice it occurs.

The ghost modification is localized on the boundaries of the worldsheet, but can be used to introduce important physical effects that at first glance are non-local on the worldsheet.

- A massive propagator requires the additional factor

$$e^{-T\mu^2/2p^+} = \lim(1 - a\mu^2/2mM)^N$$

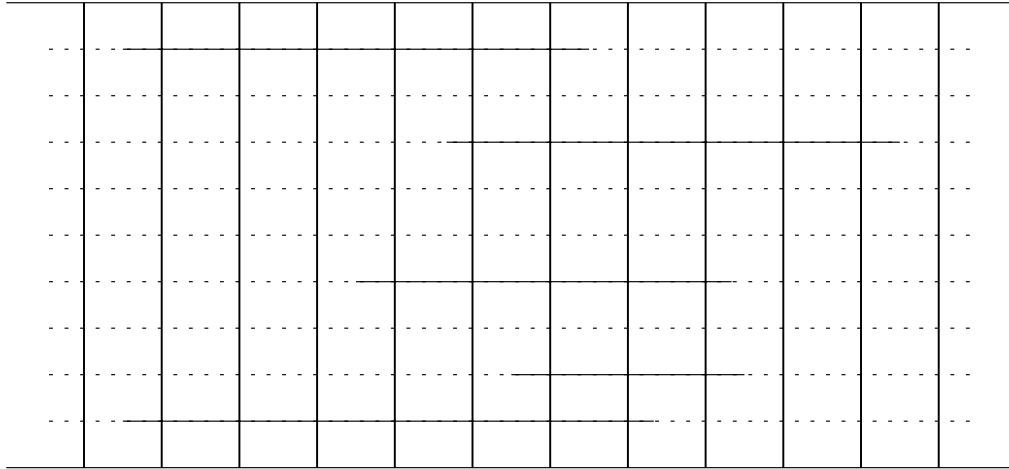
which will be produced by choosing

$$\xi = 1, \quad \text{and} \quad \eta = 1 - a\mu^2/2m$$

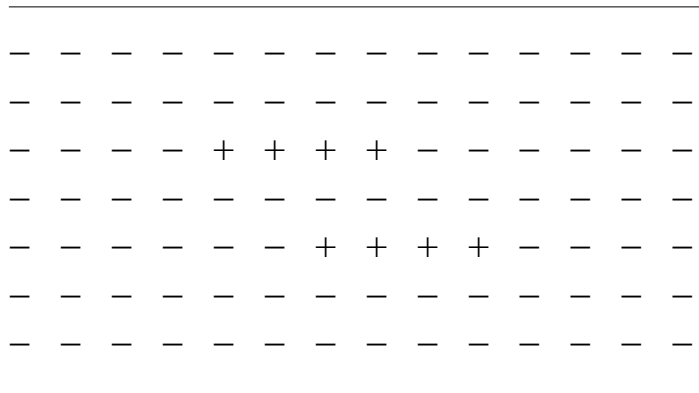
- A factor  $m/p^+ = 1/M$  must be inserted at the beginning of each propagator. This can be produced by choosing either  $\xi = 1, \eta = \infty$  or vice versa on the initial time-slice of the propagator, depending on which boundary is at the interaction point.

# Worksheet Diagram on $x^+, p^+$ Grid:

$$\sigma = im, \tau = ja$$



- Ising-like spin at each site:  $s_i^j = \pm 1$
- $P_i^j \equiv \frac{1+s_i^j}{2} = 0, 1$
- Internal boundaries (solid lines) correspond to a row of + spins. Bulk (dotted lines) is a sea of - spins. For example



is a two loop diagram.

- A factor of coupling  $g$  for each spin flip along a horizontal line.

$$\text{Number of flips} = \sum_{ij} \frac{1 - s_i^j s_i^{j+1}}{2}$$

- Dirichlet b.c.'s on solid lines:

$$\frac{P_i^j P_i^{j-1} a}{2m\epsilon} (\mathbf{q}_i^j - \mathbf{q}_i^{j-1})^2;$$

$\epsilon \rightarrow 0$  forces b.c.'s.

- Can identify an effective dynamical tension

$$\frac{P_i^j P_i^{j-1} a^2}{m^2 \epsilon} \sim T_{eff}^{-2}(s),$$

(Ising spin dependent) string tension.

Cf. AdS radius ( $\phi$ ) dependence of tension in AdS/CFT correspondence on light-cone:

$$p^- = \frac{1}{2} \int_0^{p^+} d\sigma [\mathcal{P}^2 + e^{2\phi} \mathbf{x}'^2 + e^\phi (\Pi_\phi^2 + \phi'^2)]$$

## 7 Worldsheet System for $\phi^3$

$$\begin{aligned}
 T_{fi} &= \lim_{\epsilon \rightarrow 0} \sum_{s_i^j = \pm 1} \int DcDbDq \\
 &\exp \left\{ \ln \hat{g} \sum_{ij} \frac{1 - s_i^j s_i^{j-1}}{2} - \frac{d}{2} \ln(1 + \rho) \sum_{i,j} P_i^j \right\} \\
 &\exp \left\{ -\frac{a}{2m} \sum_{i,j} \left[ \frac{P_i^j P_i^{j-1}}{\epsilon} (\mathbf{q}_i^j - \mathbf{q}_i^{j-1})^2 + (\mathbf{q}_{i+1}^j - \mathbf{q}_i^j)^2 \right] \right\} \\
 &\exp \left\{ \frac{a}{m} \sum_{i,j} \left[ A_{ij} \mathbf{b}_i^j \mathbf{c}_i^j + C_{ij} (\mathbf{b}_{i+1}^j - \mathbf{b}_i^j) (\mathbf{c}_{i+1}^j - \mathbf{c}_i^j) \right] \right\} \\
 &\exp \left\{ \frac{a}{m} \sum_{i,j} \left[ -B_{ij} \mathbf{b}_i^j \mathbf{c}_i^j - D_{ij} (\mathbf{b}_{i+1}^j - \mathbf{b}_i^j) (\mathbf{c}_{i+1}^j - \mathbf{c}_i^j) \right] \right\}
 \end{aligned}$$

- $A_{ij}, B_{ij}, C_{ij}, D_{ij}$  are Polynomials in the spin variables  $s$  or  $P$  located within 2 lattice steps from  $(i, j)$ .

## Definitions:

$$DcDbDq \equiv \prod_{j=1}^N \prod_{i=1}^{M-1} \frac{d\mathbf{c}_i^j d\mathbf{b}_i^j}{2\pi} d\mathbf{q}_i^j$$

$$P_i^j \equiv \frac{1 + s_i^j}{2}; \quad \rho = \frac{\mu^2 a}{md - \mu^2 a}; \quad \hat{g}^2 = \frac{g^2}{64\pi^3} \left[ \frac{m}{2\pi a} \right]^{\frac{d-4}{2}}$$

$$A_{ij} = \frac{1}{\epsilon} P_i^j P_i^{j-1} + P_i^{j+1} P_i^j - P_i^{j-1} P_i^j P_i^{j+1} + \\ (1 - P_i^j)(P_{i+1}^j + P_{i-1}^j) + \rho(1 - P_i^j)P_{i-1}^{j-1}P_{i-1}^j$$

$$B_{ij} = (1 - P_i^j)P_i^{j-1}P_i^{j-2}P_{i+1}^j + \\ (1 - P_i^j) \left( P_{i+1}^j P_{i+1}^{j+1} (1 - P_{i+1}^{j-1}) + P_{i-1}^j P_{i-1}^{j+1} (1 - P_{i-1}^{j-1}) \right)$$

$$C_{ij} = (1 - P_i^j)(1 - P_{i+1}^j)$$

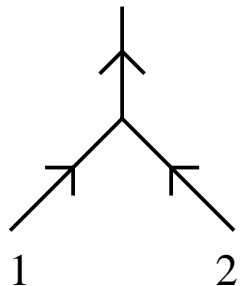
$$D_{ij} = (1 - P_i^j)(1 - P_{i+1}^j)P_i^{j-1}P_i^{j-2}$$



## Comments:

- Worldsheet system that sums QFT planar diagrams is a two-dimensional dynamical system of scalar fields  $\mathbf{q}(\sigma, \tau)$ , Grassmann ghosts  $\mathbf{b}(\sigma, \tau)$ ,  $\mathbf{c}(\sigma, \tau)$ , and Ising spins  $s(\sigma, \tau)$ .
- These degrees of freedom have a fairly complicated but *local* worldsheet action.
- The scalar and ghost fields enter the worldsheet action quadratically, but with coefficients that depend on the Ising spins.
- The role of “string tension” in this worldsheet system is played by a quantity that depends on the Ising spin configuration. Its “value” fluctuates locally and can’t be regarded as a fixed parameter.
- The fluctuating string tension is the crucial difference between the string description of a field theory and the Nambu-Goto string. We can hopefully trace the well-known short-comings of the Nambu-Goto string for describing hadrons to this difference.

# 8 Gauge Cubic Vertex

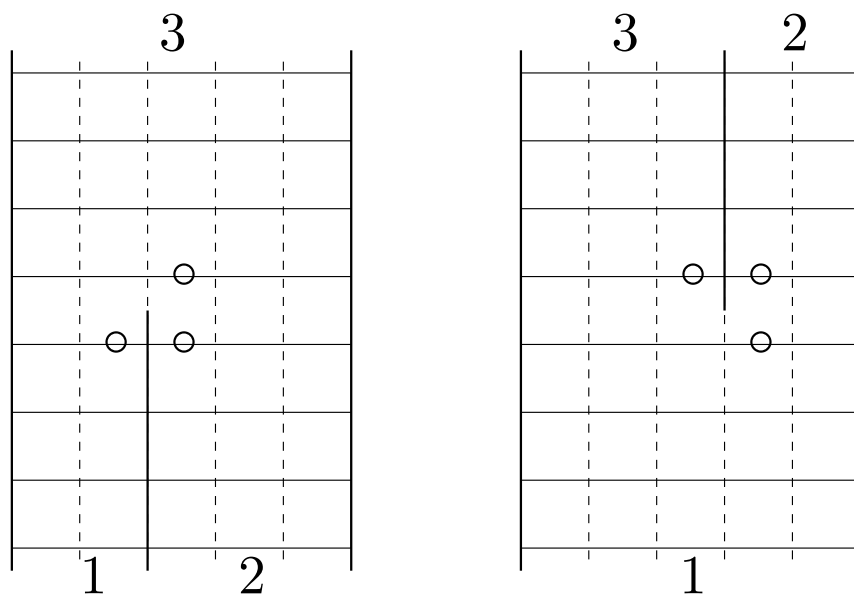


$$= \frac{ga}{4m\pi^{3/2}} p_3^+ \left( \frac{p_2^\wedge}{p_2^+} - \frac{p_1^\wedge}{p_1^+} \right)$$

Here  $v^\wedge \equiv (v^1 + iv^2)/\sqrt{2}$ ,  $v^\vee = (v^\wedge)^*$ .

On single time-slice of a single gluon,

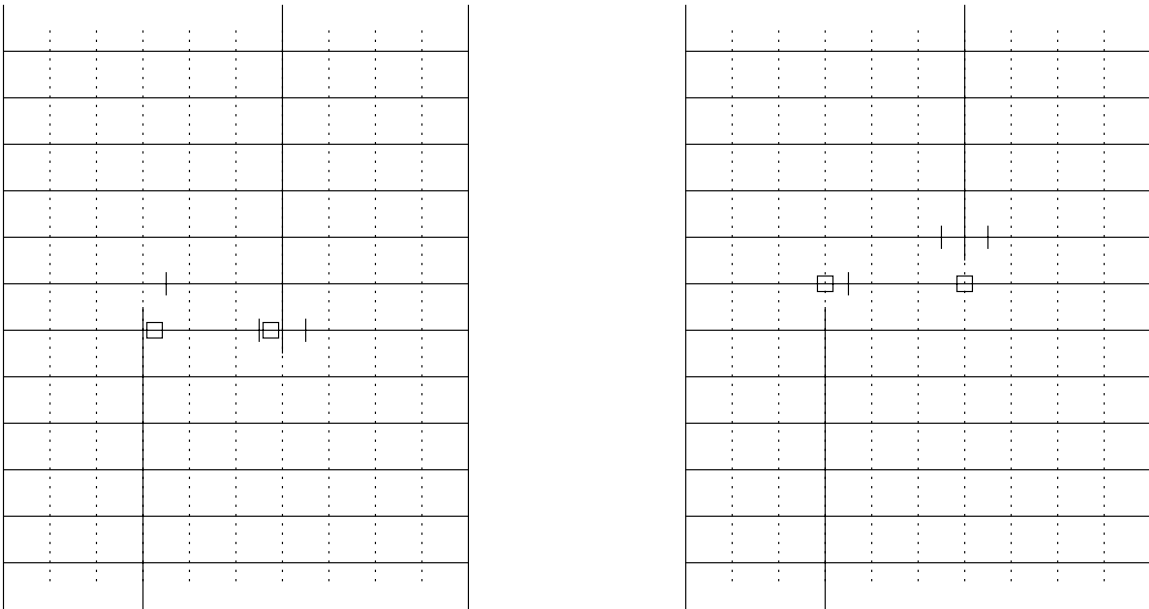
$$\langle \mathbf{q}'(\sigma) \rangle \rightarrow \frac{1}{m} \langle \mathbf{q}_l - \mathbf{q}_{l-1} \rangle = \frac{\mathbf{q}(p^+) - \mathbf{q}(0)}{p^+} = \frac{\mathbf{p}}{p^+}$$



# 9 Gauge Quartic Vertex

When  $i$  and  $j$  are on *same* time slice,

$$\frac{1}{m^2} \langle (q_{i+1} - q_i)(q_{j+1} - q_j) \rangle = \left( \frac{q(p^+) - q(0)}{p^+} \right)^2 + \frac{1}{a} \left[ \frac{1}{m} \delta_{ij} - \frac{1}{p^+} \right]$$



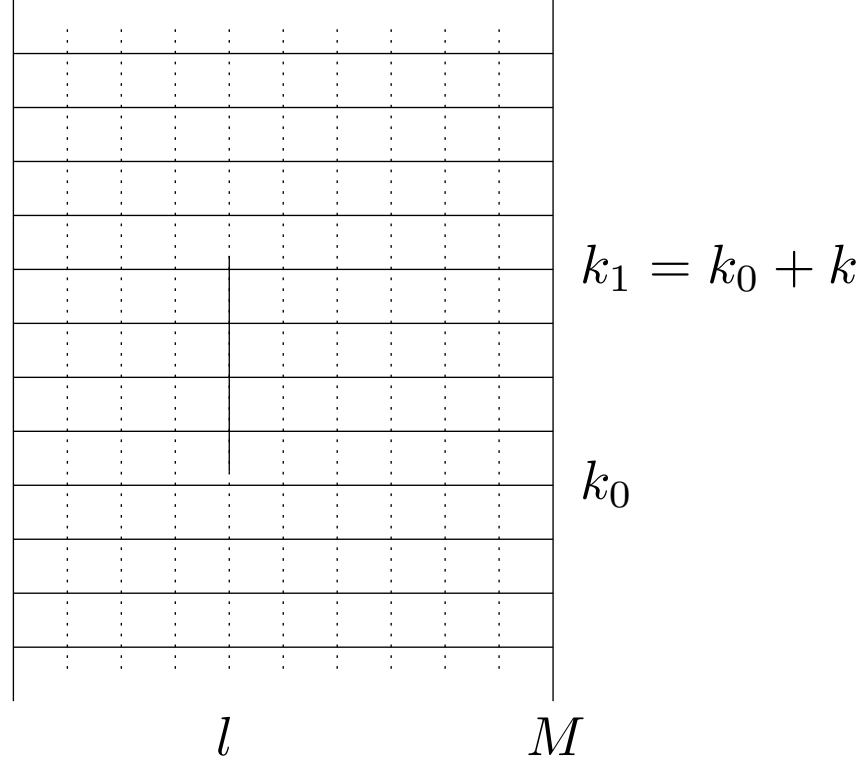
- $-\frac{1}{a} \frac{1}{p^+}$  term exactly reproduces gauge quartic vertex. This contribution allows gauge invariance to be achieved *locally* on the worldsheet.
- $\frac{1}{am} \delta_{ij}$  term is a local  $\delta(\tau)\delta(\sigma)$  worldsheet contact term.

# 10 Supersymmetry

S.Gudmundsson, C.Thorn, T.A. Tran, NPB649 (2003)  
3 hep-th/0209102

- $\mathcal{N} = 1$  SUSY: Add appropriate fermions. Everything works as with pure Yang-Mills.
- $\mathcal{N} = 2, 4$  SUSY: First add 2, 6 “dummy dimensions”.
- These dummy dimensions are given true Dirichlet b.c.’s:  $\mathbf{q}^{\text{extra}} = 0$  on all worldsheet boundaries internal as well as external.
- The fluctuations of these dummy-dimensions generates all the required quartic interactions of extended SUSY, *exactly* as in pure Yang-Mills.

# 11 One Loop Self Energy



Free propagator and counter-term

$$\begin{aligned}
 \Delta_0(q, q') &= \frac{1}{(q - q')^2 + \mu_0^2 + \alpha(\mathbf{q}^2 + \mathbf{q}'^2) + \beta(\mathbf{q} - \mathbf{q}')^2} \\
 &\equiv \sum_{n=0}^{\infty} \frac{Z^{n+1}}{[(q - q')^2 + \mu^2]^{n+1}} [\Pi_{\text{C.T.}}]^n \quad (3)
 \end{aligned}$$

$$\begin{aligned}
 \Pi_{\text{C.T.}} &= \delta\mu^2 + \left( \frac{1}{Z} - 1 \right) [(q - q')^2 + \mu^2] \\
 &\quad - \alpha(\mathbf{q}^2 + \mathbf{q}'^2) - \beta(\mathbf{q} - \mathbf{q}')^2 \quad (4)
 \end{aligned}$$

Put  $g = Z^{3/2}g_0$ , and find

$$\begin{aligned}
Z\Pi_0 &= \frac{g^2}{(4\pi)^3} \int_0^\infty \frac{dT}{(T + \delta)^2} \int_0^1 dx \\
&\quad \exp \left\{ -T \left[ \mu^2 + x(1-x)(q - q')^2 \right] \right\} \\
&\quad \exp \left\{ -\frac{\delta T}{T + \delta} (x\mathbf{q} + (1-x)\mathbf{q}')^2 \right\} \\
&\equiv \frac{g^2}{(4\pi)^3} \int_0^\infty \frac{dT}{(T + \delta)^2} \int_0^1 dx e^{-TH}
\end{aligned}$$

Integrate by parts

$$\begin{aligned}
Z\Pi_0 &= -\frac{g^2}{(4\pi)^3} \int_0^\infty \frac{dT}{T + \delta} \int_0^1 dx \left[ H_0(e^{-HT} - e^{-\mu^2 T}) \right. \\
&\quad \left. + \frac{\delta^2 (x\mathbf{q} + (1-x)\mathbf{q}')^2}{(T + \delta)^2} (e^{-HT} - 1) \right] - Z\Pi_{\text{C.T.}}
\end{aligned}$$

$$\begin{aligned}
Z\Pi_{\text{C.T.}} &= -\frac{g^2}{(4\pi)^3} \left\{ \frac{1}{\delta} - \int_0^1 dx \left[ H_0 I(\mu^2 \delta) \right. \right. \\
&\quad \left. \left. + \frac{1}{2} (x\mathbf{q} + (1-x)\mathbf{q}')^2 \right] \right\}
\end{aligned}$$

$$H_0 \equiv \mu^2 + x(1-x)(q - q')^2$$

$$I(t) \equiv \int_0^\infty \frac{e^{-ut} du}{1+u} \quad \widetilde{t \rightarrow 0} \quad \ln \frac{1}{t}$$

$$\begin{aligned} \Pi^{(1)} &\equiv Z(\Pi_0 + \Pi_{\text{C.T.}}^{(1)}) \\ &\underset{\delta \rightarrow 0}{\widetilde{}} \frac{g^2}{(4\pi)^3} \int_0^1 dx H_0 \ln \frac{H_0}{\mu^2} \end{aligned}$$

which is finite and Lorentz covariant, depending only on  $(q - q')^2$ .

At finite  $\delta$ ,  $\Pi_1$  depends also on  $\mathbf{q}$  and  $\mathbf{q}'$ . The large momentum behavior of  $\Pi_1$  is quadratic, even with  $q - q'$  fixed. This ruins power counting when inserted on propagators. For this reason we perturb about a more general propagator

$$\frac{Z}{\mu^2 + (q - q')^2 + \epsilon(\mathbf{q}^2 + \mathbf{q}'^2)}, \quad (5)$$

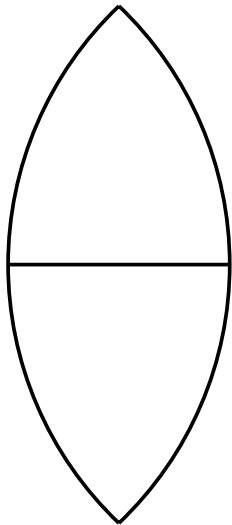
with fixed  $\epsilon$ . We only set  $\epsilon = 0$  at the end of the calculation. The changes are

$$\Pi^{(1)} \underset{\delta \rightarrow 0}{\widetilde{}} \frac{g^2}{(4\pi)^3} \int_0^1 dx H_\epsilon \ln \frac{H_\epsilon}{\mu^2}$$

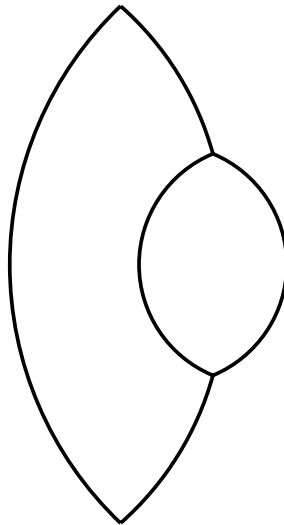
$$\begin{aligned} H_\epsilon &= \mu^2 + x(1-x)(q - q')^2 + \epsilon[x\mathbf{q}^2 + (1-x)\mathbf{q}'^2] \\ &\quad + \frac{\epsilon}{1+\epsilon}(x\mathbf{q} + (1-x)\mathbf{q}')^2 \end{aligned}$$

$$\Pi_{\text{C.T.}}^{(1)} = + \frac{g^2}{(4\pi)^3} \left\{ \frac{1}{(1 + \epsilon)\delta} - \int_0^1 dx \left[ H_\epsilon \frac{I(-\mu^2\delta/(1 + \epsilon))}{(1 + \epsilon)^2} + \frac{1}{2(1 + \epsilon)^3} (x\mathbf{q} + (1 - x)\mathbf{q}')^2 \right] \right\}$$

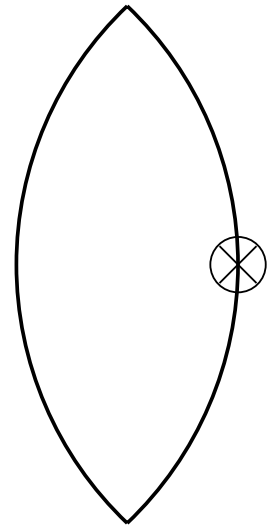
## 12 Two Loops



(a)



(b)



(c)



# 13 Conclusions

- Worldsheet “template” for planar diagrams has been set up for a whole range of interesting theories, including QCD.
- QFT UV divergences require counterterms, which (hopefully) have a *local* WS description.  
WS locality limits counterterms on Light-cone  
(Not limited by QFT locality)
- Possible computational break-through: Monte Carlo studies of the worldsheet system for QCD give a new numerical attack on large  $N_c$  QCD.